THERMODYNAMIC TREATMENT OF HIGH ENERGY HEAVY ION COLLISION

Wedad Al-Harbi

Physics Department, Sciences Faculty for Girls, King Abdulaziz University
21589 Jeddah, Saudi Arabia

Tarek Hussein

Physics Department, Faculty of Science, Cairo University
12613 Giza, Egypt

The hadron production in heavy ion collision is treated in the framework of thermodynamic vision. Thermodynamic system formed during central collision of Pb–Pb at high energies is considered, through which binary collision is assumed among the valence quarks. The partition function of the system is calculated; accordingly the free available energy, the entropy and the chemical potential are calculated. The concept of string fragmentation and defragmentation is used to form the newly produced particles. The average multiplicity of the newly produced particles are calculated and compared with the recent experimental results.

1. Introduction

In a wide energy range, there are some common aspects of heavy ion reaction dynamics. The energies are large enough and the masses of ions are also large to consider the heavy ions as classical particles. Their De Broglie wavelength is much lower than the typical nuclear sizes. Quantum effects influence the underlying microscopic dynamics only, which can be included in the equation of state, in the transport coefficients, or in the kinetic theory describing the reactions. During the collision and assuming straight line trajectories, there can be target and projectile spectators in a collision [1–3]. The rest of the nucleons may hit each other on the way forming a participant zone with both target and projectile nucleons in it. The most interesting

phenomena and the new physics are in the participant zone. The spectator regions also provide us with interesting phenomena. Realistically, the nucleons do not propagate along exactly straight trajectories. Deviations from straight propagations are observed even at the highest energies of 200 GeV per nucleon. According to the fluid dynamical model, considerable collective sideward motion is generated [4]. We shall deal with the collision problem using statistical physics concepts according to the following vision.

A heavy ion reaction is a dynamical system of a few hundred nucleons. This is a large number but still far from the continuum, so that deviations from infinite matter limit are important. On the other hand, the number of particles participating in a reaction is large enough that the signs of collective matter like behavior can be clearly observed. This is an interesting territory in statistical physics of small but collective systems. The methods developed in this field are unique and may also be applicable in other "small" statistical systems.

However, when Quark-Gluon Plasma is formed, the number of quanta increases to a large extent [5, 6]. The plasma can already be considered as a continuum, and finite particle effects should be small.

On the other hand, the heavy ion reaction is a rapid dynamical process. The question of phase transitions in a dynamical system is still an open field of research. Heavy ion physics may contribute to this field at two points: *(i)* the dynamics of the phase transitions in "small" systems, and *(ii)* the dynamics of the phase transitions in ultra-relativistic systems where the energy of the system is much higher than the rest mass of the particles.

In this context, we shall deal with the problem from the statistical thermodynamic point of view. In other words, a hypothetical model will be tailored according to the following concepts:

(a) During the heavy ion collisions, the participant nucleons form a thermodynamic system by a cylindrical cut of the projectile through the target nucleus.

(b) A fireball oriented trend is used considering valence quarks of the nucleons as the constituent particles of the overlap region.

(c) Binary collisions are assumed among the existing valence and the created sea quarks. Accordingly, a significant increase in energy density of the system leads to an environment eligible to create more particles in a frame of grand canonical ensemble.

(d) A simple quark wave function is assumed to be used in calculating the partition function of the system.

(e) A power series expansion of the partition function is assumed and we will consider only the first few terms that fit the boundary conditions of the system.

According to the above mentioned assumptions, we calculate the newly created particle multiplicity produced in Pb+Pb collisions to be compared with the recently published experimental data. In doing this, we should take into consideration the following points:

(i) The leading baryon is hardly stopped;

(ii) In the rapidity region between the projectile and the target, secondary charged particles (mesons π^+; π^-; π^0; K^+; K^-, *etc.*) are created through a string mechanism [7, 8].

The paper is organized in four sections after this soft introduction. In Sec. 2 we represent the geometry and the formulation of the model. Results and discussion are given in Sec. 3. Eventually conclusive remarks are given in Sec. 4.

2. Thermodynamic treatment of the nuclear system

In the hard sphere model, one effective radius $r = 0.4$ fm [9, 10] is chosen for all quark collisions. Elastic and inelastic collisions are considered which are supposed to be dominant at temperatures $T \approx 120$–200 MeV. The calculations are done in the framework of the Boltzmann equation with the Boltzmann statistical distribution functions and the real gas equation of state [1, 11].

The Boltzmann equation is used to find the distribution function in phase space of the thermodynamic system. It is a function in space coordinate, momentum and time. In a system of large number of particles and a special form of interaction potential, it will be difficult to get a perfect full solution of the equation. However, many trials were done [1] to get approximate solution to the Boltzmann equation in a form of conversing power series. The first term represents the equilibrium state (zero order term). The next terms represent the higher order corrections to describe the shift due to the non-equilibrium state. These terms are time dependent and include a time parameter that measure how far from the equilibrium states the particles are produced. On putting the time parameter tends to zero, all the higher terms of the series vanish and the system approaches equilibrium, and are described only by the zero order term. Another trial to find phase space distribution function in a pre-equilibrium state is the following.

Due to the non-equilibrium state, the temperature is not homogeneous all over the system, but instead there will be a temperature gradient with minimum entropy. The approach is to divide the system into small stripes (subsystems), each of its local equilibrium with a specific temperature and local equilibrium distribution. The overall phase space distribution will be the sum over the distributions of the subsystems. This is what we have done in our calculation.

The Boltzmann statistical approximation allows one to conduct precise numerical calculations of transport coefficients in the hadron gas and to obtain some relatively simple relativistic analytical closed-form expressions.

For particles having spin, the differential cross sections were averaged over the initial spin states and summed over the final ones.

The local equilibrium distribution functions are

$$f_k^0 = e^{\left(\mu_k - p_k^\mu U_\mu\right)/T}, \tag{2.1}$$

where μ_k is the chemical potential of the kth particle species, T is the temperature and U_μ is the relativistic flow 4-velocity such that $U_\mu U^\mu = 1$ with frequently used consequence.

The distribution functions f_k are found by solving the system of the Boltzmann equations approximately with the form [1]

$$f_k = f_k^0 + f_k^1 = f_k^0 + f_k^0 \varphi(x, p_k). \tag{2.2}$$

Because analytical expressions for the collision brackets are bulky, the Mathematica was used for symbolical and some numerical manipulations [12]. The numerical calculations are done also for temperatures above $T = 120$ MeV.

Let us consider the case of the binary collisions between quarks of the thermodynamic system that has been formed during the interaction of heavy ions. The total Hamiltonian is

$$H_{\mathrm{tr}} = \frac{1}{2M} \sum_{i-1}^{N} P_i^2 + \sum_{i \neq j} W_{ij}(r_{ij}), \tag{2.3}$$

where p_i is the momentum of the ith quark and W_{ij} is the binary interaction potential energy among quarks i and j.

The static quark potential at fixed spatial separation have been obtained from an extrapolation of ratios of the Wilson loops to infinite time separation. As we have to work on still rather coarse lattices and need to know the static quark potential at rather short distances (in lattice units), we have to deal with violations of rotational symmetry in the potential. In our analysis of the potential, we take care of this by adopting a strategy used successfully in the analysis of static quark potentials [13] and heavy quark free energies [14].

This procedure removes most of the short distance lattice artifacts. It allows us to perform fits to the heavy quark potential with the 3-parameter approach.

The quark–quark potential is given as

$$W_{qq}(r) = -\frac{\alpha}{r} + \sigma r + c\,. \tag{2.4}$$

The quark potential is graphically represented in Fig. 1. It is formed by 3 terms. The first is a Coulomb-like; the second is string repulsive potential that works in confinement with the quarks inside the nucleon bag.
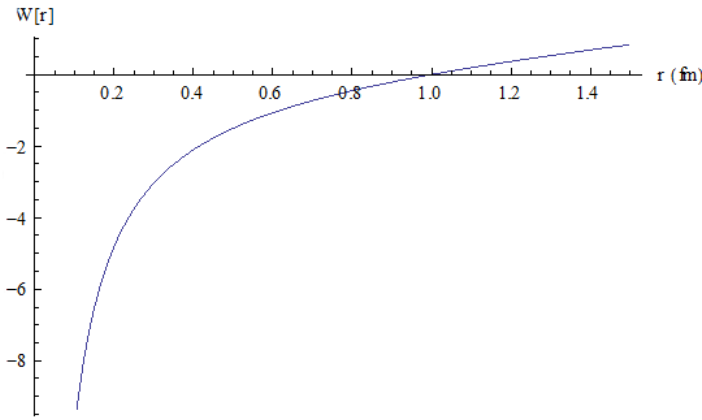

Fig. 1. 3-parameter quark–quark binary potential.

In this model, the number of created particles depends on the available energy. Accordingly, we focus our calculation on getting information about the relation between the energy and the number of interacting particles and, consequently, the number of created particles

The grand canonical ensemble considers a large supersystem kept at constant temperature and pressure and consists of many subsystems that can exchange not only the energy but also the number of particles. A number of particles and their quantum numbers corresponding to their energy states specify a microstate in the grand canonical ensemble. The particle abundance during the heavy ion collision is much complicated and depends mainly on an environment in the presence of catalyst necessary for the particle creation. The available energy is necessary to create excess of quark–antiquark pairs. Not all the quarks have the chance to form particles. Only those quarks experiencing special conditions in presence of the colored field will form a particle that satisfies the selection rules. Moreover, the strength of the color field depends on the separation distance r_{ij} .

The number of parton pairs is $\frac{1}{2}N(N-1)$ and may be approximated as $\frac{1}{2}N$ for large values of N. N depends mainly on the available energy required for creation of quark–quark pairs. We follow the thermodynamic regime that starts by calculating the partition function and the translational partition function is then

$$Z_{\mathrm{tr}} = \int \cdots \int \prod_j^{3N} \Psi_j^* e^{-H_{\mathrm{tr}}/KT} \Psi_j dq_j / h \,. \tag{2.5}$$

For the sake of indistinguishability, we divide Eq. (2.5) by $N!$ and write $Z_{\mathrm{tr}} = Z_p Z_q$ for the momentum p and spatial space q. As usual, by integration over p, we get

$$Z_p = \frac{1}{N!} \left(\frac{2\pi MkT}{h^2} \right)^{3N/2} \simeq \left(\frac{e}{N} \right)^N \left(\frac{2\pi MkT}{h^2} \right)^{3N/2} , \tag{2.6}$$

while the integration over q is not simple V^N due to the presence of the potential energy W_{ij}, which means that W_{ij} breaks the factorizability of Z

$$Z_q = \int \cdots \int \prod_j^{3N} \Psi_j^* e^{-\sum W_{\mathrm{tr}}/KT} \Psi_j dq_j / h \,. \tag{2.7}$$

Notice that for the confinement property of the potential, the potential energy has then trivial effect at small values of r_{ij}, so it is possible to write Eq. (2.7) as

$$\begin{aligned} Z_q &= \int \cdots \int \prod_j^{3N} \Psi_j^* \left[1 + \exp\left(-\sum W_{ij}/kT \right) - 1 \right] \Psi_j dq_j \\ &= V^N + \int \cdots \int \prod_j^{3N} \Psi_j^* \left[1 + \exp\left(-\sum W_{ij}/kT \right) - 1 \right] \Psi_j dq_j \,. \end{aligned} \tag{2.8}$$

For the case where $W_{ij}/kT \ll 1$, we can expand the exponential in Eq. (2.8) as $\exp[W_{ij}/kT] - 1 \approx -W_{ij}/kT$. This is applied when $r_{ij} \prec 2\, r_0$, where r_0 is the quark radius ($r_0 = 0.4$ fm). On the other hand, if W_{ij}/kT is not too small, we can consider higher order terms in the expansion of the exponential in Eq. (2.8), while for $r_{ij} \succeq 2\, r_0$, the potential increases with r i.e. positively large so that $\exp[W_{ij}/kT] \approx 0$ at extreme large values of r. Then,

$$Z_q = V^N - \tfrac{1}{2} N^2 V^{N-1} \left[4\pi \int_{2r_0}^{R} \Psi_1^* \left[1 + \exp(-W_{ij}/kT) - 1 \right] \Psi_1 r_{1j}^2 dr_{1j} \right] . \tag{2.9}$$

Now, it is possible to calculate $F, S, U \ldots$ for this system in terms of Z. $F = -NkT(\ln Z - \ln N + 1)$. The entropy $S = -(\partial F / \partial T)_{N,V}$, then

$$S = NkT \left(\frac{\partial \ln Z}{\partial T} \right)_V + Nk(\ln Z - \ln N + 1). \qquad (2.10)$$

The internal energy $U = F + TS$; then,

$$U = NkT^2 \left(\frac{\partial \ln Z}{\partial T} \right)_V. \qquad (2.11)$$

The total internal energy U is the important physical quantity in the model and is directly related to the energy density and the particle multiplicity production. The wave function Ψ_j is assumed to be very similar to that used by the parton model. Starting with the simplest parametric form of the quark wave function

$$\widetilde{\Psi}_a(p) = Ce^{-\alpha p}, \qquad a \succ 0, \qquad p \succeq 0, \qquad (2.12)$$

and p is the null momentum in the parton model [15, 16]. The Fourier transform of the quark wave function is then

$$\Psi(r) = \frac{C'}{(r + ia)^2}, \qquad (2.13)$$

where C and C' are normalization constants, while a is a fitting parameter. Again, inserting Eq. (2.13) into Eq. (2.5) gives the total energy of the quark assembly of the nucleons. The range of the null momentum p extends from zero up to $P_{\max}$. It is more convenient to express the wave function and all other physical quantities in terms of the Bjorken scaling variable with $x = P/P_{\max}$ lies in the range of $0 \prec x \prec 1$. Particle creation through formation and fragmentation of quarks is used through the string model [17], consequently, the multiplicity of particle creation is calculated and compared with the recent results of Pb–Pb collisions at incident momentum per nucleon of 40, 80 and 158 GeV. (Experiment: CERN-NA-049 (TPC) [18–21].)

3. Results and discussion

We consider the case of central collisions in heavy ions of Pb–Pb. Let us assume that overlap region at impact parameter b has a cylindrical form. The number of nucleons and, consequently, the number of quarks N_n-part

and N_q-part for Pb+Pb collisions are calculated as [22]

$$
N_{n-\text{part}}|_{AB} = \int d^2 S T_A\left(\vec{S}\right)\left[1-\left(1-\frac{\sigma_{NN}^{\text{inel}}T_B\left(\vec{S}-\vec{b}\right)}{B}\right)^B\right]
$$
$$
+ \int d^2 S T_B\left(\vec{S}\right)\left[1-\left(1-\frac{\sigma_{NN}^{\text{inel}}T_A\left(\vec{S}-\vec{b}\right)}{A}\right)^A\right] , \quad (3.1)
$$

where $\sigma_{NN}^{\text{inel}}$ is the inelastic nucleon–nucleon cross section and $T(b) = \int_{-\infty}^{\infty} dz$ $n_A(\sqrt{B^2 + Z^2})$ is the thickness function. In calculating $N_{q-\text{part}}$, the density was increased three times and $\sigma_{NN}^{\text{inel}}$ is replaced by $\sigma_{qq}^{\text{inel}}$. We concentrate our calculation on the central collision region, where $b \preceq R_P + R_T \sim 6$ fm. On the average, the number of nucleons (quarks) in the considered region is 250 (750). Figure 2 illustrates the participant number of nucleons (quarks) according to the Glauber calculation [22].
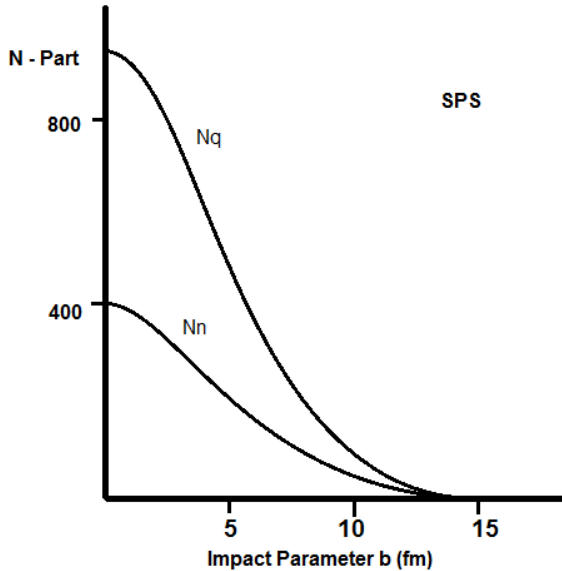

Fig. 2. Number of participant nucleons (quarks) in the overlap region as a function of the impact parameter b for the Pb–Pb collision.

The partition function for N particles is calculated according to Eq. (2.9) for separation distance r_{ij} of the binary interacting quarks. The family of curves of the partition function represented in Fig. 3 corresponds to temperature 20, 40, 60 and 200 MeV. The temperature is very sensitive to the form
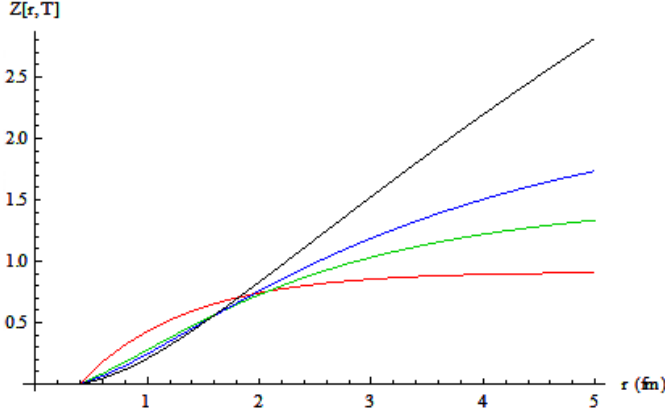
Fig. 3. The partition function $Z(r,T)$ as a function of the separation distance between the interacting quarks. Different curves belong to temperature values of (20 (gray/red), 40 (light gray/green), 60 (dark gray/blue) and 200 (black) MeV).

of the nuclear density and increases as the number of participant nucleons from the projectile N_P and the target nucleus N_T come close ($N_P \longrightarrow N_T$). The temperature of the system is determined according to the impact parameter and, consequently, depends on the number of participating nucleons (quarks) [1]

$$\zeta_{\text{cm}} = 3T + m\frac{K_1(m/T)}{K_2(m/T)}, \tag{3.2}$$

$$\zeta_{\text{cm}} = \left[m^2 + 2\eta(1-\eta)mt_{\text{i}}\right]^{1/2}. \tag{3.3}$$

In Eq. (3.2), ζ_{cm} represents the relativistic form of the center-of-mass energy of a system of temperature T (using system of units where the Boltzmann constant $K = 1$). The first term on the l.h.s., ($3T$ or $3kT$) is the thermal energy. The second term is the relativistic correction [1]. In Eq. (3.3), $\zeta_{\text{cm}} = [m^2 + 2\eta(1-\eta)mt_{\text{i}}]^{1/2}$ describes also the center-of-mass energy for the particles in the overlap region of projectile and target having nuclear densities ρ_P and ρ_T respectively with relative projectile density $\eta(r,b)$ at position coordinate r and impact parameter b [1] defined as

$$\eta(r,b) = \frac{\rho_P(r,b)}{\rho_P(r,b) + \rho_T(r,b)}. \tag{3.4}$$

Solving the two equations (3.2) and (3.3), it is possible to find the temperature T at any r and b. t_{i} is the incident kinetic energy per nucleon. K_1 and K_2 are the Macdonald functions of first and second order. At low

temperature $T \sim 20$ MeV, the partition function $Z(r,T)$ approaches flat behavior just above $r_{ij} \simeq 2$ fm. At higher temperature $(T = 40\ 60$ MeV), the r_{ij} dependence of $Z(r,T)$ becomes steeper. Approximate linear behavior is found at high temperature $T = 200$ MeV.

On the other hand, the smooth variation of $Z(r,T)$ over all the range of temperature $T, 20 \longrightarrow 200$ MeV is given in Fig. 4 with family of curves corresponding to $r_{ij} \sim 2, 3, 4, 5$ and 6 fm. A steep drop of $Z(r,T)$ is observed in the cold region $(T < 20$ MeV) for all curves of $r_{ij} \sim 2, 3, 4, 5$ and 6 fm. This is followed by smooth increase toward the hot region up to $T \sim 200$ MeV.
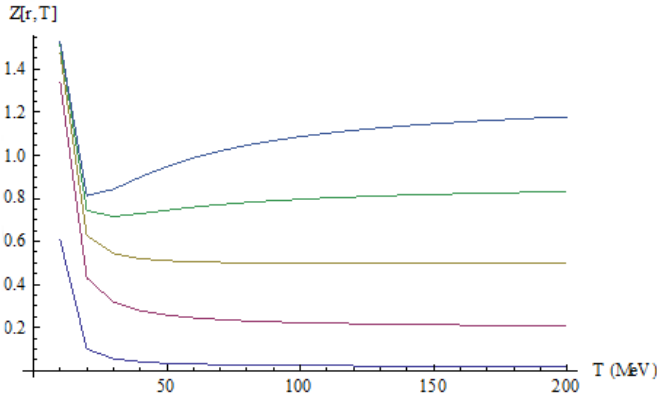

Fig. 4. The behavior of the partition function $Z(r,T)$ in a temperature range up to 200 MeV.

The changes of the partition function express the behavior of the quark chemical potential μ inside the hadronic system through the well known relation: $\mu = -kT \ln Z$.

Figure 5 shows the change of quark chemical potential in a temperature range up to 200 MeV. The total energy $U(r)$ dissipated in the nuclear interaction region due to the binary quark collisions is represented in Fig. 6 in the temperature range of $T < 200$ MeV. The curves are plotted for quark–quark separation distances $r_{ij} \sim 2, 3, 4, 5$ and 6 fm. $U(r)$ has positive values in the small range of $r_{ij} \sim 2, 3, 4$ fm, where the quarks are approximately free and can carry enough energy to create particles. However, $U(r)$ has negative values in the large range of $r_{ij} \sim 5$ and 6 fm, where the quarks are mostly confined by the string potential.

A Monte Carlo program is used to simulate the particle production in the frame of the String Model [17]. The particle production is considered as a tunneling process in a colored field. Because of the 3-gluon coupling, the color flux lines will not spread out over the space as the electromagnetic field lines do but rather be constrained to a thin tube like region. Within this
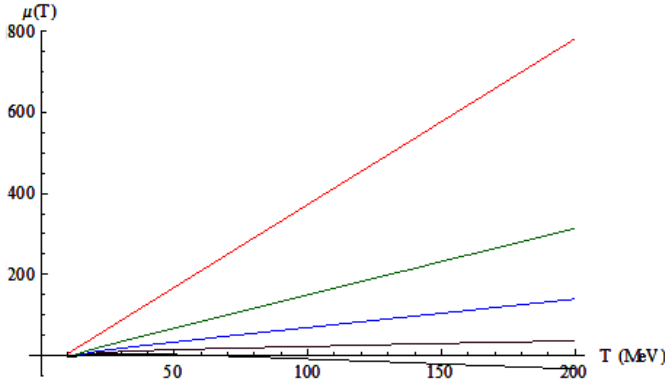
Fig. 5. The change of quark chemical potential in a temperature range up to 200 MeV.
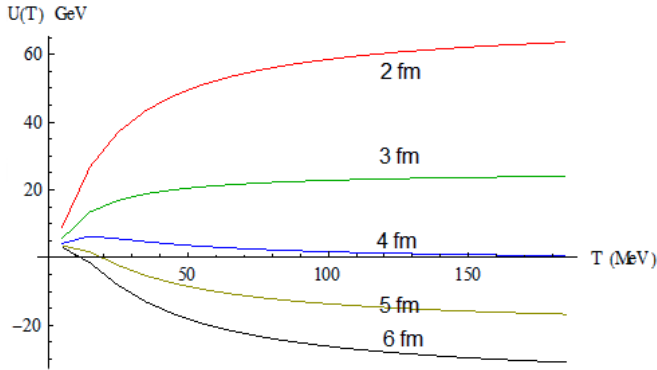

Fig. 6. (Color online) The total potential energy formed inside the nuclear system in the temperature range $T < 200$ MeV. The curves are plotted for quark separation distances $r_{ij} \sim 2$ (red), 3 (green), 4 (blue), 5 (yellow) and 6 (black) fm.

tube, new $q\bar{q}$ pairs can be created from the available field energy. The original system breaks into smaller pieces, until only ordinary hadrons remain. In the field behind the original outgoing quark q_0, a new quark pair $q_1\bar{q}_1$ is produced so that the original one q_0 may join with a new one $\bar{q}_1$ to form a hadron $q_0\bar{q}_1$ leaving $\bar{q}_1$ unpaired. The production of another pair $q_2\bar{q}_2$ will give a hadron $q_1\bar{q}_2$, *etc.* From this assumption one may find the resulting particle spectra in a jet. The possible meson formations by the quark pairs are presented in Table I. The simulation process allows the production of all types of mesons with all possible branching ratios taking into account the selection rules and the conservation laws.

TABLE I

All possible $q\bar{q}$ pairs with their probable meson type formation.

$q\bar{q}$	Spin J	Meson probability		
$u\bar{u}$	0 1	$P(\pi^0) = 0.5$ $P(\rho^0) = 0.5$	$P(\eta^0) = 0.25$ $P(\omega^0) = 0.5$	$P(\eta') = 0.25$
$u\bar{d}$	0 1	$P(\pi^+) = 1$ $P(\rho^+) = 1$		
$u\bar{s}$	0	$P(K^+) = 1$		
$d\bar{u}$	0 1	$P(\pi^-) = 1$ $P(\rho^-) = 1$		
$d\bar{d}$	0 1	$P(\pi^0) = 0.5$ $P(\rho^0) = 0.5$	$P(\eta^0) = 0.25$ $P(\omega^0) = 0.5$	$P(\eta') = 0.25$
$d\bar{s}$	0	$P(K^0) = 1$		
$s\bar{s}$	0 1	$P(\eta^0) = 0.5$ $P(\omega^0) = 0$	$P(\eta') = 0.5$ $P(\phi) = 1$	
$s\bar{u}$	0	$P(K^-) = 1$		
$s\bar{d}$	0	$P(K^0) = 1$		

In Table II, the prediction of the simulation shows overall fair agreement. In most cases at energies 20 and 30 A GeV, the thermodynamic model prediction exceeds the measured value by 11–15%. The prediction of the model for pions and kaons at energy 158 A GeV gives values a little bit under estimation with respect to the experimental values. However, the calculated value for the ϕ particle gives unexpected result (double the experimental value), this may be due to the fact that the ϕ comes from the channel of $s\bar{s}$ quarks. In our model, the production of u, d and s pairs were considered equally probable; this seems in contrast to the real case.

Unfortunately, the Monte Carlo code, used in our calculations, was designed by our research group in 1995 [17]. In this code, the charged particles (mesons π^+; π^-; π^0; K^+; K^-, *etc.*) are created through string mechanism and the recombination of the specific quarks, irrelevant of the mechanism of production whether due to the decay of resonance particle ($K*$, ...) or not. We are working right now to develop this code, taking into consideration most of the recent information.

On the other hand, the recent STAR measurements on the production of various strange hadrons (K^0s, phi, Lambda, Xi and Omega) in $\sqrt{S_{NN}} = 7.7$–39 GeV Au+Au collisions show that strange hadron productions are sensitive probes to the dynamics of the hot and dense matter created in heavy ion

TABLE II

Yields of particle production at Pb–Pb collisions at 20 and 30 and 158 A GeV. The measured data are taken from Refs. [20, 21] for pions and kaons only. The possible measured values are compared with the prediction of the present model.

Average particle production	20 A GeV		30 A GeV		Ref.	158 A GeV		Ref.
	Measured data	Prediction of the model	Measured data	Prediction of the model		Measured data	Prediction of the model	
$\langle \pi^- \rangle$	221.0 ± 1	250.4	274 ± 1	311.1	[20]	639 ± 45	540	[21]
$\langle \pi^0 \rangle$		140.0		197.6			301	
$\langle \pi^+ \rangle$	190.0 ± 1	211.6	241.0 ± 1	183.7	[20]	619 ± 45	510	[21]
$\langle K^+ \rangle$	40.7 ± 0.7	35.5	52.9 ± 0.9	70.3	[20]	103 ± 7	100	[21]
$\langle K^- \rangle$	10.3 ± 0.1	15.3	16.0 ± 0.2	40.2	[20]	51.9 ± 3.6	73	[21]
$\langle \rho^0 \rangle$		5.4		11.5			43	
$\langle \rho^+ \rangle$		2.6		6.1			34	
$\langle \rho^- \rangle$		3.5		4.3			37	
$\langle \omega^0 \rangle$		1.7		2.0			28	
$\langle \eta^0 \rangle$		1.3		2.1			25	
$\langle \phi \rangle$						8.46 ± 0.5	20	[21]

collisions. The extracted chemical and kinetic freeze-out parameters with the thermal and blast wave models as a function of energy and centrality were studied and discussed by Zhu [23, 24].

We also believe that hadron production is, in general, a good probe to study hadron formation mechanism in heavy ion collisions. At high transverse momentum, p_T, the hard processes, which can be calculated with perturbative QCD, are expected to be the dominate mechanism for hadron productions. It was observed at RHIC that, at high p_T, the RCP (the ratio of scaled particle yields in central collisions relative to peripheral collisions) of various particles [25] indicates dramatic energy loss of the scattered partons in the dense matter (jet quenching). RCP of hadrons have been measured also at SPS [26, 27], though the limited statistics restricts the measurement at relatively lower p_T (0.3 GeV/c). Measuring the nuclear modification factor in heavy ion collisions at this energy range, one can potentially pin down the beam energy at which interactions with the medium begin to affect hard partons [28].

4. Conclusive remarks

— New particles need special environment to be produced during the heavy ion collisions.

— Multiple collisions among the quarks of the nuclear system should produce large enough energy compared with the particle chemical potential. The strong colored field plays the role of a catalyst parameter necessary for particle production.

— The free available energy $U(r)$ has positive values in the small interaction distance, where the quarks are approximately free and can carry enough energy to create particles. However, $U(r)$ has negative values in the large interaction distance, where the quarks are mostly confined by the string potential.

— The string fragmentation and defragmentation is applied for the production of the different types of newly produced particles.

— Theoretical attempts to understand the energy dependence of the suppression were undertaken. Calculations were based on the Glauber–Gribov model, in which the energy-momentum conservation was implemented into the multiple soft parton re-scattering approach.

— The temperature is very sensitive to the form of the nuclear density. The temperature increases as the number of participant nucleons from the projectile N_P and the target nucleus N_T come close.

— The temperature of the system is determined according to the impact parameter and, consequently, depends on the number of participating nucleons (quarks).

— The thermodynamic model prediction exceeds the measured value by percentage 11–15%.

— The quark–hadron phase transition will be studied in a forthcoming article through a temperature-quark chemical potential phase diagram.

REFERENCES

[1] M.T. Hussein, N.M. Hassan, N. El-Harby, *Turk. J. Phys.* **24**, 501 (2000); J. Gosset *et al.*, *Phys. Rev.* **C16**, 629 (1977); J. Gosset, J.I. Kapusta, G.D. Westafall, *Phys. Rev.* **C18**, 844 (1978); W.D. Myers, *Nucl. Phys.* **A296**, 177 (1978).

[2] M.T. Hussein, N.M. Hassan, N. El-Harby, *Acta Phys. Hungarica N.S. Heavy Ion Phys.* **13**, 277 (2001).

[3] Huichao Song *et al.*, *Phys. Rev.* **C83**, 054910 (2011).

[4] ALICE Collaboration, *Phys. Lett.* **B696**, 328 (2011).

[5] A.V. Nefediev, Yu.A. Simonov, *Phys. Atom. Nucl.* **71**, 171 (2008).

[6] J.-P. Blaizot, *J. Phys. G* **34**, S243 (2007).

[7] Q.-G. Huang, *Phys. Rev.* **D74**, 063513 (2006).

[8] M.N. Chernodub, F.V. Gubarev, *Phys. Rev.* **D76**, 016003 (2007).

[9] S.N. Syritsyn *et al.*, *Phys. Rev.* **D81**, 034507 (2010).

[10] M.I. Gorenstein, M. Hauer, O.N. Moroz, *Phys. Rev.* **C77**, 024911 (2008).

[11] Y. Mizutani, T. Inagaki, *Prog. Theor. Phys.* **125**, 933 (2011).

[12] http://www.wolfram.com

[13] R. Sommer, *Nucl. Phys.* **B411**, 839 (1994).

[14] O. Kaczmarek, F. Karsch, F. Zantow, P. Petreczky, *Phys. Rev.* **D70**, 074505 (2004).

[15] M.T. Hussein, A.I. Saad, *J. Mod. Phys.* **1**, 244 (2010).

[16] M.T. Hussein, N.M. Hassan, W. Elharbi, *Int. J. Mod. Phys.* **A18**, 673 (2003).

[17] M.T. Hussein, A. Rabea, A. El-Naghy, N.M. Hassan, *Prog. Theor. Phys.* **93**, 585 (1995).

[18] N. Davis *et al.* [NA49 Collaboration], *Phys. Atom. Nucl.* **75**, 661 (2012).

[19] G.L. Melkumov *et al.* [NA49 Collaboration], *Nucl. Phys. Proc. Suppl.* **219-220**, 102 (2011).

[20] NA49 Collaboration, *Phys. Rev.* **C77**, 024903 (2008).

[21] F. Becattini *et al.*, *Phys. Rev.* **C85**, 044921 (2012).

[22] M.K. Hegab, M.T. Hussein, N.M. Hassan, *Z. Phys.* **A336**, 345 (1990).

[23] X. Zhu, *Acta Phys. Pol. B Proc. Suppl.* **5**, 213 (2012).

[24] X. Zhu [STAR Collaboration], *Nucl. Phys.* **A830**, 845c (2009).

[25] J. Rafelski, B. Muller, *Phys. Rev. Lett.* **48**, 1066 (1982).

[26] B.I. Abelev *et al.*, *Phys. Rev.* **C77**, 044908 (2008).

[27] J. Adams *et al.*, *Phys. Rev. Lett.* **98**, 062301 (2007).

[28] X. Wang [STAR Collaboration], *J. Phys. G* **35**, 104074 (2008).